Self-Assembly and Stress Relaxation in Acrylic Triblock Copolymer Gels

Michelle E. Seitz, Wesley R. Burghardt, K. T. Faber, and Kenneth R. Shull*

Department of Materials Science and Engineering, Northwestern University, Evanston, Illinois 60208

Received August 29, 2006; Revised Manuscript Received December 7, 2006

ABSTRACT: The structure and relaxation behavior of thermoreversible gels made with poly(methyl methacrylate)−poly(*n*-butyl acrylate)−poly(methyl methacrylate) [PMMA−PnBA−PMMA] triblock copolymers in 2-ethylhexanol, a midblock selective solvent, were studied by small-angle X-ray scattering (SAXS) and rheology. Effects of endblock length, endblock fraction, and gel concentration on the gel properties were investigated. A dramatic decrease in SAXS intensity was observed over a 20 °C interval where the gel transitions smoothly from elastic to viscous behavior. SAXS patterns were fit with a Percus−Yevick disordered hard-sphere model from which aggregation number and average domain spacing were calculated. Aggregation number increases with increasing gel concentration and endblock length. Increasing the endblock length from 9K to 25K increases the relaxation time of a gel with a polymer volume fraction of 0.15 by a factor of 10^6. For a given triblock endblock fraction and molecular weight, the micelle aggregation number is strongly correlated to the gel relaxation time. Arrhenius behavior with an effective activation energy of ∼550 kJ/mol was observed for all triblocks and concentrations. This very high effective energy barrier describes gels relaxation behavior over a 40 °C temperature range, where the relaxation times vary by a factor of 10^{10}.

Introduction

Symmetric ABA triblock copolymers are of both theoretical and practical importance because of their ability to self-assemble into ordered structures. Their technological importance is due to their ability to form elastic solids via self-assembly, with midblocks bridging aggregated endblock micelles.[1] When triblock copolymers are dissolved in a midblock selective solvent, they form gels that retain many desirable properties of the liquid phase while adding the ease of handling and robust nature of an elastic solid. Additionally, the thermoreversible nature of the gel transition makes these systems ideal from a processing perspective. Styrene-based triblock systems are used as thermoplastic elastomers,[2] as pressure-sensitive adhesives,[3] and as substrates for microfluidic systems.[4] Recently, acrylic triblock copolymer gels have been investigated as a novel processing route for ceramics[5,6] as well as for model pressure-sensitive adhesives.[7,8] Triblocks in liquid crystal solvents take advantage of the homogeneity produced by self-assembly to form elastic solids with rapid switching times and excellent optical properties.[9] Aqueous systems with hydrophilic midblocks and short hydrogenated or fluorinated hydrophobic endblocks are used as thickening agents in surface coatings and cosmetics, oil recovery, and wastewater treatment.[10,11] Triblock hydrogels with poly(lactide) endblocks are of interest for tissue engineering because their modulus is similar to that of soft tissue.[12]

Thermoreversibility of triblock gels originates from the temperature dependence of the interaction parameter between the endblocks and the solvent, χ_{AS}. Temperature-driven gel formation is shown schematically in Figure 1. For systems that lack long-range ordering of micelles, two transition temperatures are important. The first of these is the critical micelle temperature (cmt) where the endblock aggregates, commonly referred to as micelles, form. As the gel is cooled, the solvent quality for the endblocks worsens and solvent is expelled from the aggregates.[13] The second transition is the glass transition (T_g) of the still slightly swollen endblock domains. Systems that rely on endblock crystallization to form network cross-links have much slower gelation kinetics than systems governed by glass transitions.[13] PMMA−PnBA−PMMA triblocks in alcohols are a particularly useful system because the cmt is generally less than 100 °C and the endblock glass transition is typically above room temperature, although both transition temperatures have block length and concentration dependence. As a result, an elastic gel with an extremely long relaxation time is formed at room temperature.[13] The very rapid, thermally reversible liquid−solid transition makes this system of interest for materials processing applications.[5,6]

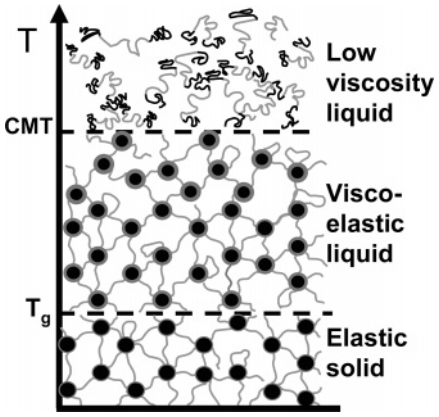

Figure 1. An illustration of the temperature-dependent structure of acrylic triblock copolymer gels in alcohols adapted from Drzal and Shull.[13]

In contrast, aqueous systems tend to gel on heating[14] and lack the long relaxation times[15] of acrylic or styrenic gels. Commercially available poly(styrene)−poly(ethylene-*co*-butylene)−poly(styrene) [SEBS] triblocks form thermoreversible gels in mineral oils; however, they have a broader transition between liquid and solid behavior,[16] and the nonvolatile nature of the

* Corresponding author. E-mail: k-shull@northwestern.edu.

10.1021/ma061993+ CCC: $37.00
Published on Web 01/24/2007

solvent is undesirable for materials processing applications where castings must be dried prior to sintering. Also, acrylic gels have viscosities low enough for casting at much lower temperatures than SEBS systems. For gels with similar molecular weight, endblock fraction, and overall polymer concentration, the viscosity of acrylic gels is reduced to 0.1 Pa s at 75 °C,[13] compared to 200 °C[17] for SEBS gels.

In order to optimize the acrylic gels for processing applications, we need to understand the parameters that control the gel behavior. If the relaxation time is too short at low temperature, the solid character of gels necessary for molding applications will be lost. Conversely, large relaxation times at high temperatures will give viscosities that are too high for the material to be poured into a mold. In this paper we describe the connection between endblock fraction and molecular weight, gel structure, and viscoelasticity of PMMA−PnBA−PMMA gels in 2-ethylhexanol of various concentrations.

Background

Block copolymers are simple systems that satisfy the two requirements for self-assembly: short-range attractive forces (A−B covalent bonds) and long-range repulsive forces (A−B repulsions).[18] The structure formed depends on the balance between interfacial tension and the chain stretching entropy. Depending on the relative volume fraction of each block, neat diblock copolymers form spherical, cylindrical, gyroid, and lamellar phases[19] with the feature size determined by block length. The phase space for symmetric triblock copolymers is similar to that of diblocks since they share the same driving force for aggregation, which for spherical and cylindrical geometries can be viewed as micelles.[20] Spherical micelles are formed when the endblocks are short relative to the midblocks. Ordering of block copolymers in selective solvents is similar to the ordering of neat copolymers, except that the solvent−polymer interactions are generally the dominant driving force for micellization. Depending on the strength of the polymer−solvent interactions, the micelle core will be solvated to some degree. Whether the micelles exhibit only short-range order or long-range order depends on processing history and represents a competition between micelle ordering and physical network formation.[21,22] Long-range order is favored at higher polymer concentration[22,23] and may develop if the gel is annealed at temperatures where the endblocks are able to exchange.[16,24] Micelle size does not appear to change as micelle long-range order develops.[16] Ordering was not observed in any of the acrylic triblock copolymer gels investigated in this paper, and thus the discussion will focus on systems exhibiting only short-range order.

The crucial difference between diblock and triblock copolymers is the opportunity for midblocks to form either loops or bridges in triblock systems. Unentangled looped chains do not carry stress whereas bridges and interlocking loops can transmit stress between connected micelles and contribute to the shear modulus. From rubber elasticity theory, the shear modulus, G, for an ideal Neohookean material that has been isotropically swollen by solvent is given by[25]

$$G = \nu k_B T \frac{d^2}{{R_0}^2} = f\left(\frac{\varphi_p \rho RT}{M}\right)\frac{d^2}{{R_0}^2} \quad (1)$$

where ν is the number density of elastically active chains, d is the average distance between cross-links, ${R_0}^2$ is the mean-squared end-to-end distance for an equilibrium solution of molecules with a molecular weight equal to the average molecular weight between cross-links, f is the fraction of elastically active molecules, φ_p is the polymer volume fraction, M is the polymer molecular weight, and ρ is the polymer density. For triblock copolymer gels, d scales with the average distance between aggregates and reflects stretching of the midblocks due to geometric constraints. For triblock copolymer gels with a midblock concentration in the unentangled regime, eq 1 describes the modulus.[26]

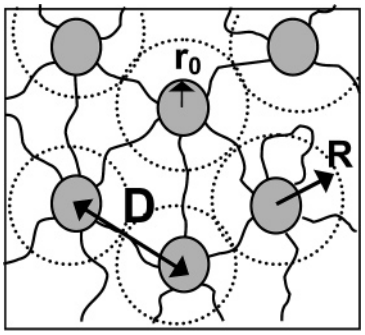

Figure 2. Gel structure in the elastic state. Endblock cores are located an average distance, D, apart. The micelle core has a radius, r_0, and is surrounded by a fictitious hard sphere of radius R.

In a triblock gel, the number of elastically active chains, and therefore the modulus, increases with an increase in the ratio of bridges to loops. For a solution of diblock micelles $f = 0$, while f can vary in triblock gels. Monte Carlo simulations of triblocks in midblock selective solvents[14,27,28] as well as experimental dielectric studies[29] have shown that the number of bridges increases with polymer concentration. Self-consistent-field theory calculations for triblock melts find a bridging fraction of about 0.8 for spherical micelles.[20] For highly concentrated solutions, most chains would be expected to be in a bridged conformation due to the entropic penalty associated with forcing both endblocks to reside in the same micelle. Semenov's theoretical treatment invoking an analogy to planar brush layers shows that triblock micelles strongly attract each other and that the number of bridges scales with the micelle aggregation number and the concentration of micelles in solution.[30]

Many theoretical studies have investigated micellization in block copolymers. Leibler, Orland, and Wheeler's free energy approach to calculating the critical micelle concentration (cmc) of diblock copolymers in homopolymer solvent[31] has been extended to diblock copolymers[32] and triblock copolymers[33] in a selective solvent. These studies focus on scaling relationships between block length, core and corona radius, and aggregation number. An increase in aggregation number with concentration for triblocks in selective solvents has been seen experimentally for styrene-based systems[34] and in theoretical studies.[28,35] This behavior differs from what is observed in dilute solutions of surfactants or copolymers[36] and in Pluoronic systems in water.[37] In these cases an increase in concentration is accommodated by creating more micelles, not by increasing the aggregation number.

Figure 2 represents the structure of a triblock gel below the critical micelle temperature. Triblock gels can be modeled as a random distribution of hard spheres in a liquid.[8,21,24,38,39] Each fictitious hard sphere of radius R contains a micelle core of radius r_0. The final parameter describing the system is the volume fraction of hard spheres, η. The aggregation number, g, or number of endblocks per micelle core, is given by the

number of endblocks divided by the number of micelles in a given volume:

$$g = \left(\frac{2\rho\varphi_p N_{av}}{M}\right)\left(\frac{4\pi R^3}{3\eta}\right) \quad (2)$$

where ρ is the polymer density, φ_p is the polymer volume fraction in the gel, N_{av} is Avogadro's number, and M is the total triblock molecular weight. The average distance between micelle cores, D, is given by

$$D = \left(\frac{4\pi R^3}{3\eta}\right)^{1/3} \quad (3)$$

From eq 2 it is clear that as φ_p increases two mechanisms can accommodate the new polymer chains: either the average spacing between micelles can decrease, or the aggregation number can increase. An increase in average spacing between micelles requires bridged midblocks to be more stretched and therefore will favor loop formation.

In conditions where the endblocks are able to exchange between aggregates, e.g., above the glass transition of the aggregates and when the solvent is not too poor for the endblock, triblock gels must technically be classified as viscoelastic liquids, although the relaxation times may be extraordinarily large. Stress is relaxed when an endblock disengages from its aggregate. Triblock gels may therefore be described using transient network theory developed for associating polymers.[40] A summary of this theory as well as its expansion to take into account the concentration dependence of elastically active chains can be found in ref 14. Briefly, endblock dissociation from aggregates arising from thermal motion or tension must overcome a potential energy barrier. Transient network theory predicts Maxwell-type viscoelastic behavior with a single relaxation time. The energy barrier depends on the incompatibility, $\chi_{AS}N_A$, between the solvent and the endblock where N_A is the degree of polymerization of the endblock. The temperature dependence of segmental mobility will further increase the effective energy barrier. Therefore, the gel relaxation time should increase with increasing endblock length and with decreasing temperature (for systems with upper critical solution behavior) since χ_{AS} is temperature dependent.

Aqueous systems of telechelic associating polymers with extremely short endblocks ($N_A < 20$) exhibit single relaxation time Maxwell-type viscoelasticity with a relaxation time that varies exponentially with hydrophobe length,[14,41] although the relaxation behavior changes when the micelles adopt long-range order.[42] Terminal relaxation behavior with the storage and loss moduli increasing with the second and first powers of the frequency, respectively, has been observed in triblock melts[2] and gels[23,43] with much longer endblocks ($N_A \sim 80-165$). At higher frequencies, the storage moduli plateau, the loss moduli do not approach a limiting slope of -1, indicating that these materials are not characterized by a single relaxation time.

Inomata et al. investigated the association behavior of a PMMA−PtBA−PMMA gel in 1-butanol as a function of temperature and concentration.[43] NMR and light scattering experiments on dilute solutions found that the triblock is molecularly dissolved at high temperatures. As temperature is reduced, the solvent quality for the endblock decreases until micellization occurs. On increasing the gel concentration, the physical network grows by incorporation of aggregates by increasing the fraction of bridging chains. Master curves were produced via time−temperature superposition, with terminal relaxation behavior observed at temperatures lower than the micellization temperature measured by light scattering. Thus, the gel behaves as a transient network able to flow at high temperature due to endblock detachment from associated cores. Inomata et al.'s study provides an excellent understanding of how the physical network develops as a function of concentration. The present work aims to expand the understanding of these types of materials by investigating the effect of endblock fraction and chain length on gel structure and relaxation behavior. The main result of this investigation is that the effective energy barrier describing the removal of a PMMA endblock from an aggregate is independent of gel concentration, endblock fraction, and overall chain length.

Table 1. Triblock Copolymers Used in This Study

polymer	A: PMMA MW [g/mol]	B: PnBA MW [g/mol]	fraction PMMA
$A_{25}B_{116}A_{25}$	25 000	116 000	0.3
$A_9B_{53}A_9$	8 900	53 000	0.23
$A_{23}B_{31}A_{23}$	23 000	31 000	0.6

Experimental Details

Materials. Gels were made by dissolving PMMA−PnBA−PMMA triblock copolymer in 2-ethylhexanol, a midblock selective solvent, above 90 °C. The triblock copolymers were provided by Kuraray Co. and were used as received. Three different triblocks with various endblock fractions and chain lengths were investigated and are summarized in Table 1. The naming convention uses A and B to refer to PMMA and PnBA blocks, respectively, with subscript numbers referring to each block's molecular weight in kg/mol. Polydispersity was obtained from size exclusion chromatography using polystyrene standards. Polydispersities for $A_{25}B_{116}A_{25}$, $A_9B_{53}A_9$, and $A_{23}B_{31}A_{23}$ were 1.39, 1.26, and 1.18, respectively.

Methods. Small-angle X-ray scattering (SAXS) experiments were performed at the DND-CAT beamline 5ID-D at Argonne National Lab's Advanced Photon Source. Room temperature gel samples were made by casting a heated solution in a washer (1.6 mm thick, 7.6 mm diameter) between two Kapton layers. Temperature ramp experiments were performed on gels loaded into 1.5 mm diameter boron-rich capillaries. Capillaries were placed in contact with a copper block inside a Linkham THMS 600 hotstage, and the temperature was recorded by a thermocouple in contact with the copper block. The samples were heated at 2 °C/min. The scattering vector ($q = 4\pi \sin\theta/\lambda$) range covered 0.1−1.0 nm^{-1} using a beam energy of 17 keV. Isotropic patterns were collected on a 2D detector and then integrated over all azimuths to generate one-dimensional data.

Rheological measurements were performed on a Paar Physical MCR-300 rheometer with a double-gap Couette (DG26.7) type fixture. Gels were heated above 70 °C and loaded into the fixture. Gels were equilibrated at each measurement temperature, and a strain sweep was performed to identify the linear viscoelastic (LVE) regime. Isothermal frequency sweeps over an angular frequency (ω) range from 0.1 to 100 s^{-1} were performed at a constant stress chosen such that the resulting strain was in the LVE regime. The temperature dependence of the dynamic moduli was measured on heating and cooling at a strain of 1%, $\omega = 10$ s^{-1}, and a heating rate of 1 °C/min. Viscosity data for neat 2-ethylhexanol and for gels above 70 °C were collected in steady rotation at a strain rate of 50 s^{-1} with a heating rate of 1 °C/min.

Swelling experiments were conducted by casting gels in washers (2.5 mm thick, 10.4 mm diameter) between glass slides. Gels were cooled, removed from the washers, weighed, and placed in a baths of pure solvent. Once the gels reached equilibrium, they were nominally dried on filter paper and then weighed. The equilibrium swelling ratios were calculated by dividing the swollen weight by the initial weight.

Results and Discussion

Small-Angle X-ray Scattering. The effect of temperature on the structure of an $A_{25}B_{116}A_{25}$ gel with $\varphi_p = 0.15$ is shown

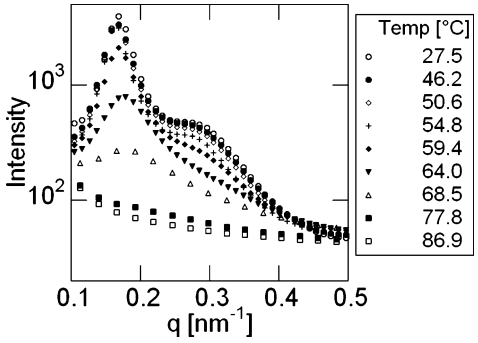

Figure 3. Scattering intensity vs q for an $A_{25}B_{116}A_{25}$ gel with $\varphi_p = 0.15$ heated at 2 °C/min.

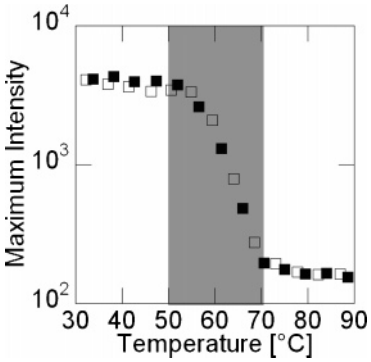

Figure 4. Maximum intensity vs temperature for an $A_{25}B_{116}A_{25}$ gel with $\varphi_p = 0.15$. Open symbols were collected on heating and closed symbols on cooling. The shaded region indicates the temperature range over which X-ray contrast from the endblock aggregates is lost.

in Figure 3. At low temperature there are clear peaks which decrease in intensity as the temperature is raised. Figure 4 plots the maximum intensity of the lowest q peak as a function of temperature. The dramatic drop in scattering intensity between 50 and 70 °C indicates reversible changes in the X-ray contrast of the sample and suggests a broad structural transition. The X-ray contrast in the gel comes from the difference in electron density between dense PMMA endblock aggregates and the well-solvated PnBA midblocks. A transition from a gel with aggregated endblocks to a polymer solution would result in a decrease in scattering intensity. However, increased solvation of endblock aggregates would also result in a decrease in X-ray contrast.

Patterns were taken at room temperature for gels with polymer volume fractions, φ_p, ranging from 0.1 to 0.3. The patterns were fit using the Percus−Yevick disordered hard-sphere model[44] in which the scattering intensity is given by

$$I(q) = KNP(q)\,S(q) \tag{4}$$

where K is a constant, N is the number of scattering centers, $P(q)$ is the particle form factor, and $S(q)$ is the structure factor. Details of the fit can be found in the literature.[8,38,39,45] The location of the low-q peaks are determined primarily by the structure factor, which depends on R, the hard-sphere radius, and η, the volume fraction of hard spheres. The peak at higher q ($q \sim 0.65$ nm^{-1}) is controlled by the particle form factor, which depends on r_0, the scattering core radius, and σ, a parameter describing the scattering center boundary diffuseness.[45] Figure 2 illustrates the physical meaning of R and r_0. Figure 5 shows the room temperature SAXS pattern for a $A_{25}B_{116}A_{25}$ gel with $\varphi_p = 0.15$ and the Percus−Yevick fit with $R = 19.3$ nm, $r_0 = 8.9$ nm, $\eta = 0.42$, and $\sigma = 1$. Values of the

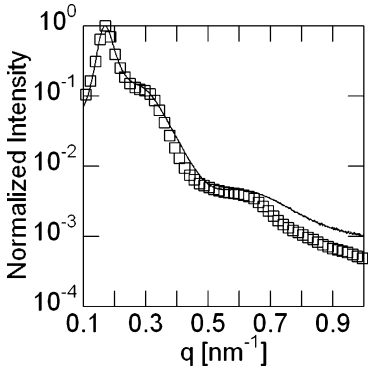

Figure 5. Normalized intensity vs q for $A_{25}B_{116}A_{25}$ gel with $\varphi_p = 0.15$ at room temperature. Open symbols are raw data, and line is Percus−Yevick fit with parameters $R = 19.3$ nm, $r_0 = 8.9$ nm, $\eta = 0.42$, and $\sigma = 1$.

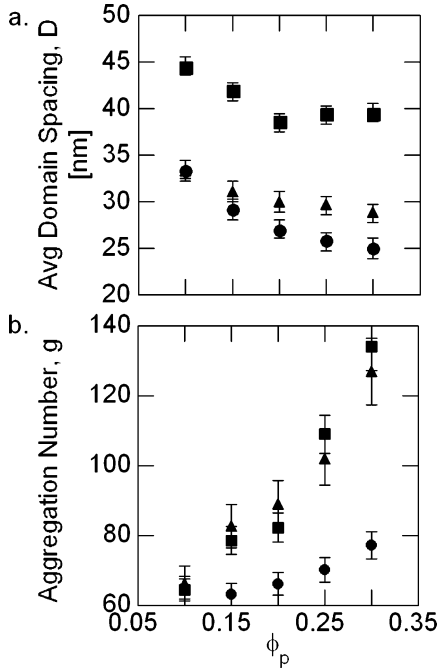

Figure 6. Average domain spacing (a) and aggregation number (b) vs polymer volume fraction, φ_p, for $A_{25}B_{116}A_{25}$ (■), $A_9B_{53}A_9$ (●), and $A_{23}B_{31}A_{23}$ (▲).

hard-sphere radius and volume fraction, which in turn determine aggregation number and average distance between cores through eqs 2 and 3, are obtained by the fit to the low q ($q < 0.5$ nm^{-1}) part of the pattern, where excellent agreement with the experimental data is achieved.

Aggregation numbers and average domain spacings calculated from the SAXS fits using eqs 2 and 3 are shown in Figure 6. Estimating average domain spacing by presuming the location of the first scattering peak is related to the Bragg spacing for micelles with bcc packing[46] yields values nearly identical to those calculated from eq 3. All three triblocks showed qualitatively similar behavior. The average domain spacing is weakly dependent on φ_p as expected for gels with well-solvated midblocks. In contrast, the aggregation number increases strongly with φ_p. As the endblock length increases, the aggregation number's dependence on concentration increases. Gels of $A_{25}B_{116}A_{25}$ and $A_{23}B_{31}A_{23}$ experience a more rapid increase in aggregation number than $A_9B_{53}A_9$ gels with much smaller endblocks but similar relative endblock volume fraction as $A_{25}B_{116}A_{25}$.

Modulus and Swelling Behavior. At low temperatures, these gels behave as viscoelastic solids at accessible frequencies, with a well-defined shear modulus. For eq 1 to apply, the gels must lack midblock entanglements. The number of entanglements per molecule, n_e, for a polymer in a good solvent is given by

$$n_e \sim N_e \varphi_p^{5/4} \tag{5}$$

where N_e is the number of entanglements per molecule in the melt.[47] Midblock entanglements are not expected to be present in our systems since the entanglement molecular weight of neat PnBA is 22 000 g/mol.[48] For $A_{25}B_{116}A_{25}$, the polymer volume fraction at which midblocks form one entanglement is 0.26, and for the other polymers studied it is higher than the experimental volume fractions investigated. It is not appropriate to use eq 1 to describe the concentration dependence of the modulus for triblock systems in the concentration range where midblock entanglements are present.[16,23,49]

Information about midblock conformations can be obtained by calculating the combined variable $f(d^2/R_0^2)$ from eq 1 using measurements of the plateau modulus. Figure 7a,b shows how both the plateau modulus measured at 30 °C and $f(d^2/R_0^2)$ vary as a function of φ_p. At high concentrations where bridge formation is favored, f should approach one for each polymer system. The dimensionless factor $f(d^2/R_0^2)$ increases when midblocks are more strongly stretched as they clearly are for $A_{23}B_{31}A_{23}$ gels at $\varphi_p > 0.15$. At lower concentrations, the increased midblock chain stretching due to larger aggregate spacing favors loop formation, which is consistent with the lower modulus of $A_{23}B_{31}A_{23}$ gels at $\varphi_p = 0.1$. The strong stretching of the midblocks for $A_{23}B_{31}A_{23}$ gels is consistent with their large aggregation numbers and relatively short midblocks. In contrast, $A_{25}B_{116}A_{25}$ gels have comparable aggregation numbers, but as expected their much longer midblocks are not strongly stretched.

Equilibrium swelling ratios for $A_{25}B_{116}A_{25}$ and $A_{23}B_{31}A_{23}$ gels immersed in pure solvent at room temperature are shown in Figure 7c. Equilibrium swelling ratios were not obtained for $A_9B_{53}A_9$ gels because their relaxation time at room temperature was shorter than the time required to reach equilibrium swelling; however, at short times they swelling behavior was similar to $A_{23}B_{31}A_{23}$ gels of the same initial concentration. For all initial concentrations, $A_{25}B_{116}A_{25}$ gels swell to several times their initial weight, indicating that their midblocks are able to deform to accommodate more solvent molecules. In contrast, $A_{23}B_{31}A_{23}$ gels either weakly shrink at low initial concentration or weakly swell at higher initial concentrations. This result is consistent with the calculated values of $f(d^2/R_0^2)$ which indicate that the midblocks of $A_{23}B_{31}A_{23}$ gels are in an extended conformation when the gel is formed. The swelling data are also consistent with $A_{23}B_{31}A_{23}$ gels having larger average domain spacing than $A_9B_{53}A_9$ gels (Figure 6a) even though $A_{23}B_{31}A_{23}$ gels have shorter midblocks.

Rheology. Temperature ramp experiments illustrate the profound change in rheology that occurs over a moderate temperature range in these samples (Figure 8). Below 50 °C, the response is highly elastic, with $G' \gg G''$. Upon heating, the $A_{25}B_{116}A_{25}$ gel ($\varphi_p = 0.15$) considered here undergoes a transition to a liquid state at ~63 °C. (We use the $G'-G''$ crossover as a convenient indicator of a gel temperature.) Above this temperature, the response is viscous dominated, with $G'' \gg G'$, and the moduli drop rapidly as the material softens into a low-viscosity liquid. This definition of the gel temperature as the temperature where the relaxation time is comparable to the time scale of the experiment is convenient in our case. It differs, however, from definitions based on the formation of a continuous percolating network. These percolation concepts are most relevant when the lifetimes of the bonds are very long, as with covalent cross-links, for example.[50] For the relatively large polymer concentrations used here, a percolating network always exists below the cmt. Previous studies estimate the glass transition for the solvated endblock aggregates in a $A_{23}B_{92}A_{23}$ gel in 2-ethylhexanol to be ~36 °C.[13]

Despite the profound structural changes revealed by SAXS as the sample passes through the gel temperature, isothermal

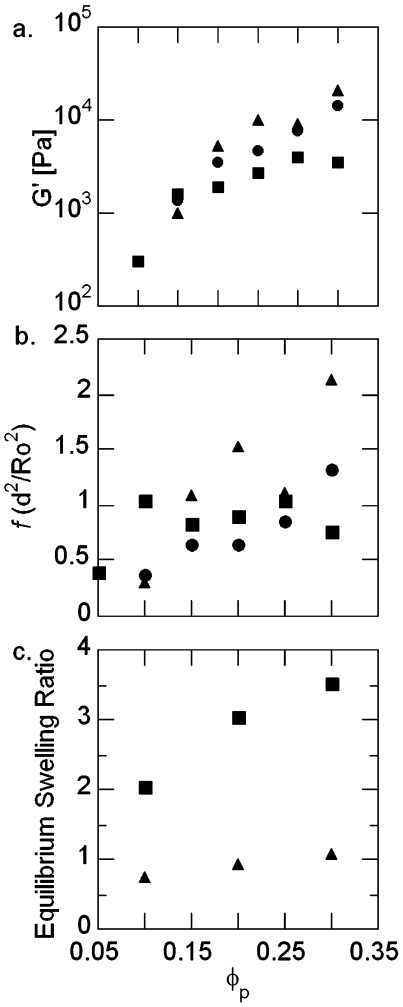

Figure 7. Dependence of (a) storage modulus, G', and (b) $f(d^2/R_0^2)$ on polymer volume fraction, φ_p, at 30 °C for $A_{25}B_{116}A_{25}$ (■), $A_9B_{53}A_9$ (●), and $A_{23}B_{31}A_{23}$ (▲) gels. (c) Equilibrium swelling ratio vs initial gel polymer volume fraction, φ_p, at room temperature.

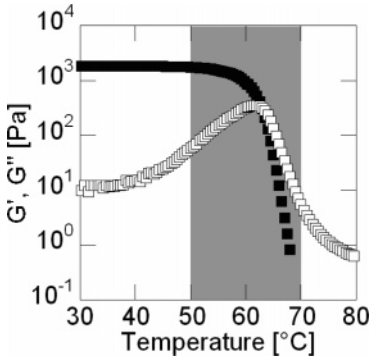

Figure 8. Temperature dependence of G' (■) and G'' (□) for an $A_{25}B_{116}A_{25}$ gel ($\varphi_p = 0.15$) heated at 1 °C/min. Shaded region corresponds to region over which SAXS intensity decreases in Figure 4.

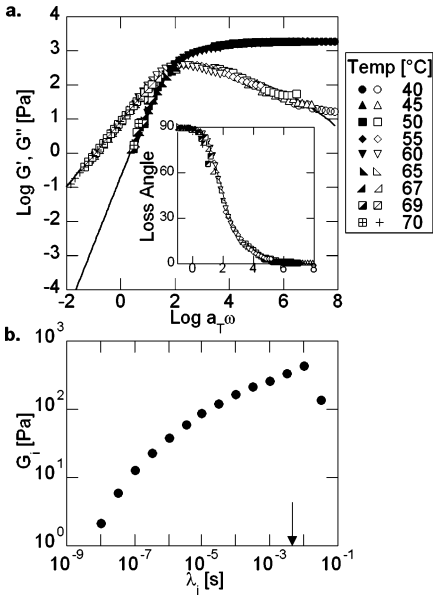

Figure 9. (a) Master curve showing G' (closed symbols) and G'' (open symbols) for $A_{25}B_{116}A_{25}$ gel with $\varphi_p = 0.15$ created by shifting frequency sweeps collected between 40 and 70 °C [reference temperature of 65 °C] along the frequency axis. Inset shows semilog plot of the loss angle's smooth transition from viscous to elastic behavior. (b) Parameters used for multimode Maxwell model shown as lines in (a**).** Arrow marks the relaxation time defined by eq 8.

frequency sweep data collected at various temperatures may be used to produce a single master curve governing the viscoelastic spectrum over this temperature range (Figure 9). (Master curves were produced by shifting along the frequency axis, with no shift along the modulus axis.) For all samples, these master curves reveal the response to be that of a viscoelastic liquid, in which the loss (G'') and storage (G') moduli approach limiting power law dependencies on ω of 1 and 2, respectively, at low frequency. At high frequency, G' becomes independent of frequency; however, G'' decreases with a power law of ~ -0.3, a smaller slope than power law of -1 predicted for a single relaxation time Maxwell model. This indicates that there is a range of times associated with endblock exchange between aggregates. Lines in Figure 9a represent a generalized Maxwell model fit to the master curve, leading to the discrete spectrum of relaxation times shown in Figure 9b. The storage and loss moduli are given by and

$$G'(\omega) = \sum_i \frac{G_i \lambda_i^2 \omega^2}{1 + \lambda_i^2 \omega^2} \tag{6}$$

$$G''(\omega) = \sum_i \frac{G_i \lambda_i \omega}{1 + \lambda_i^2 \omega^2} \tag{7}$$

λ_i and G_i are the ith mode's relaxation time and modulus.[51] Interestingly, the power law behavior of G'' at high frequency and the shape of the relaxation spectrum are similar to those observed in melts of monodisperse linear, flexible polymers in the flow regime.[52]

The loss angle varies smoothly from nearly 0° to 90°, indicating that the transition from nearly perfectly elastic behavior to viscous flow occurs smoothly over the 30 °C interval used in constructing this master plot. The temperature-dependent data in Figure 8 are thus seen to follow naturally from the time−temperature superposition of a fundamentally liquidlike relaxation spectrum.

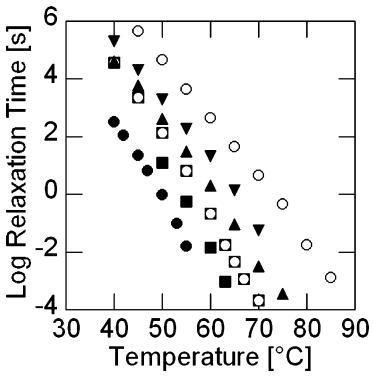

Figure 10. Temperature dependence of relaxation times for $A_{25}B_{116}A_{25}$ gels with polymer volume fraction, $\varphi_p = 0.05$ (●), 0.1 (■), 0.15 (⊡), 0.2 (▲), 0.25 (▼), and 0.3 (○).

The fact that superposition is possible suggests that the fundamental origins of viscoelasticity in these gels is not changing over this temperature range. Even though the SAXS data indicate the nature of the aggregates themselves changes dramatically over this temperature range, it appears that stress in these solutions is carried by midblock chains whose relaxation is mediated by exchange of endblocks between aggregates—a process which is very highly temperature dependent. Qualitatively similar master curves for PMMA−PtBA−PMMA in 1-butanol were obtained by Inomata et al. and show terminal relaxation behavior at temperatures where light scattering indicate that the endblocks are aggregated.[43]

Vega et al. have modeled relaxation in triblock gels with styrene endblocks and either isoprene or ethylene-*alt*-propylene midblocks using theory developed for entangled star polymers.[23] They argue that the rheological behavior in their systems is strongly affected by trapped midblock entanglements. As discussed above, midblock entanglements are not expected to significantly affect the properties of the acrylic gels studied. In addition, the similarity between the master curves generated for all polymers and concentrations suggests that midblock entanglements are not affecting the rheology of these systems.

Stress Relaxation. From the master curve for each sample we can construct a relaxation time, τ, at any given temperature using

$$\tau = \frac{\eta_0 a_T}{G_0} \tag{8}$$

where η_0 and G_0 are the zero shear viscosity and the plateau modulus determined respectively from low- and high-frequency regimes at the reference temperature, while a_T is the shift factor for the temperature of interest. The zero shear viscosity is calculated from

$$\eta_0 = \lim_{\omega \to 0} \frac{G''(\omega)}{\omega} \tag{9}$$

Figure 10 shows the temperature dependence of the relaxation time for $A_{25}B_{116}A_{25}$ gels with φ_p ranging from 0.05 to 0.3. At 60 °C, the relaxation time for this triblock increases by 5 orders of magnitude as φ_p increases from 0.1 to 0.3. For polymers $A_9B_{53}A_9$ and $A_{23}B_{31}A_{23}$, relaxation times increase by about 3 orders of magnitude over the same φ_p range. Relaxation time is also strongly affected by the endblock length. For example, $A_9B_{53}A_9$ gels with $\varphi_p = 0.15$ relax about 10^6 times faster than $A_{25}B_{116}A_{25}$ gels with the same φ_p.

Gel Temperature. Using the $G'-G''$ crossover as an indicator of a gel temperature, T_{gel}, represents the temperature at which

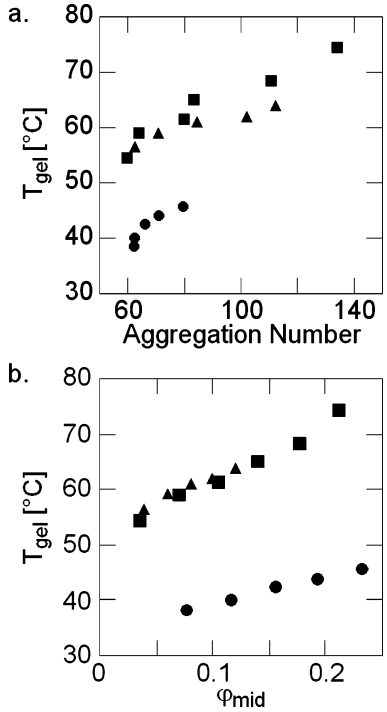

Figure 11. T_{gel} vs (a) aggregation number and (b) volume fraction of midblock, φ_{mid}, for $A_{25}B_{116}A_{25}$ (■), $A_9B_{53}A_9$ (●), and $A_{23}B_{31}A_{23}$ (▲).

the relaxation time is roughly equal to $1/\omega$. Temperature ramp tests for the gel temperature were performed with $\omega = 10\ s^{-1}$, thus probing the sample on a time scale of 0.1 s. Over a range of gel concentrations, each triblock type showed a small hysteresis in gel temperature with measurements on heating, yielding values 1−2 °C higher than on cooling. The hysteresis is small because gelation corresponds to the equilibration of the very small PMMA aggregates and not to crystallization or stereocomplexation; indeed, some of the observed hysteresis may result from thermal lag due to the finite heating/cooling rates. By contrast, triblocks with syndiotactic PMMA endblocks that form gels in *o*-xylene via endblock stereocomplexation exhibit a hysteresis in gel temperature of 20 °C.[53]

Gels made from $A_9B_{53}A_9$ had gel temperatures about 20 °C lower than gels made with either of the longer endblock materials whose gel temperatures are comparable to each other. Figure 11 shows T_{gel} against micelle aggregation number as determined by room temperature SAXS and against the volume fraction of midblocks in the gel, φ_{mid}. As the aggregation number or the volume fraction of midblocks is increased for a given triblock copolymer, T_{gel} shifts to higher temperatures.

We note here that styrenic triblock gels with additions of diblock copolymers equal to half a triblock chain produce SAXS patterns nearly identical to neat triblock gels.[23] Therefore, the addition of diblocks, even at very high concentrations, is not expected to affect the micelle aggregation number. Additionally, adding diblocks to a triblock gel does not affect the location of the gel temperature[54] which offers further evidence that T_{gel} is controlled by aggregation number. However, diblock additions do affect the bridging fraction and, therefore, the plateau modulus of the gels. The ability of diblock additions to decouple aggregation number and gel modulus might enable design of gels with specific moduli and relaxation behavior.

Relaxation Time Superposition. Shifting the relaxation spectra along the temperature axis by an amount equal to the gel temperature causes the data for all three polymers in all concentrations studied to collapse onto one curve, as shown in Figure 12. This superposition of relaxation spectra is possible because the apparent activation energy, ΔH_{app}, for removing an endblock from an aggregate is similar for all samples investigated. Arrhenius plots of the shift factor, a_T, vs $1/T$ were used to determine ΔH_{app}. All samples had $\Delta H_{app} \approx 550$ kJ/mol, which describes the temperature dependence throughout the 30−40 °C temperature range that could be accessed for a given sample. Our results are consistent with values of the apparent activation energy between 450 and 568 kJ/mol, reported for PMMA−PtBA−PMMA gels in 1-butanol.[43] However, this value is much higher than the ∼200 kJ/mol value observed for systems with styrene endblocks.[2,23] Aqueous systems of poly(ethylene oxide) chains with short hydrophobic endblocks[14] have an activation energy of ∼70 kJ/mol, valid over a 60 °C temperature range.

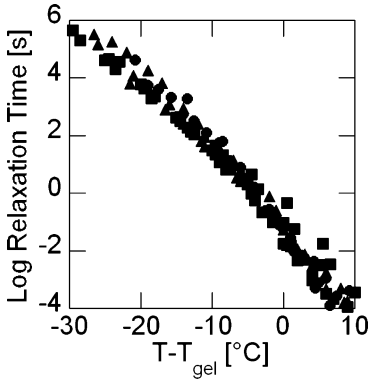

Figure 12. Superposition generated by shifting relaxation spectra along the temperature axis by their gel temperatures for gels of $A_{25}B_{116}A_{25}$ ($\varphi_p = 0.05-0.3$) (■), $A_9B_{53}A_9$ ($\varphi_p = 0.1-0.3$) (●), and $A_{23}B_{31}A_{23}$ ($\varphi_p = 0.1-0.3$) (▲).

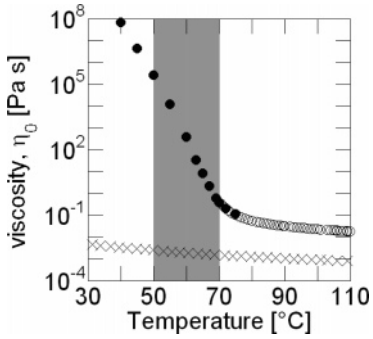

Figure 13. Viscosity vs temperature 2-ethylhexanol (×) and for an $A_{25}B_{116}A_{25}$ gel ($\varphi_p = 0.15$). Viscosities calculated using the time−temperature superposition of master curves of oscillatory data are shown as closed circles while viscosities measured in steady rotation are shown as open circles. The shaded area corresponds to temperature region where the SAXS intensity decreases in Figure 4.

If the strong temperature dependence shown in Figure 12 is a result of endblock exchange between aggregates, it must level off at temperatures above the cmt when the endblock aggregates dissociate. Figure 13 shows that there is a slope change in the viscosity vs temperature curve. At higher temperatures, the viscosity of the triblock solution parallels that of the pure solvent as expected for polymer solutions.[51] The enhancement in viscosity closely corresponds with the temperature at which aggregate formation is just becoming noticeable in the SAXS data.

The temperature dependence of χ_{AS} contributes to both the thermodynamic and kinetic portions of the large apparent energy barrier observed in this paper and by Inomata et al.[43] Since χ_{AS} increases with decreasing temperature, the energy penalty for removing an endblock from an aggregate also increases with

decreasing temperature. Additionally, the mobility of the endblocks decreases with decreasing temperature because they are nearing their glass transition. The location of this glass transition is at least partly controlled by the degree of solvation of the endblocks which again must depend on χ_{AS}.

The attempt frequency for endblock disengagement will depend on the mobility of the endblocks. This frequency will be affected by the volume fraction of solvent within an aggregate, $\varphi_{S,A}$, because solvation plasticizes the endblock aggregates. Since the chemical potential of the solvent is uniform through the system, $\varphi_{S,A}$ will also depend upon the concentration of solvent in contact with the solvated midblocks. Changing the overall gel concentration might affect the mobility of endblocks within an aggregate and therefore the gel relaxation time by changing $\varphi_{S,A}$. Since solvent plasticization would affect the glass transition temperature of the aggregates, it might be possible to detect this effect by careful determination of the aggregate's glass transition using probe techniques.[55]

It is remarkable that a universal scaling of relaxation times over 10 orders of magnitude is possible for systems with vastly different aggregations number, block lengths, and gel concentrations. The degree to which aggregation number affects the relaxation behavior of a gel depends on the particular triblock endblock fraction and chain length. Although the gel temperature and aggregation number are strongly affected by the endblock length and gel concentration, the effective energy barrier is insensitive to them. This suggests the effective energy barrier is determined by the interaction between the solvent and the PMMA segments.

Conclusions

The structure and relaxation behavior as a function of endblock fraction and chain length, gel concentration, and temperature for PMMA−PnBA−PMMA triblock copolymer gels in 2-ethylhexanol have been investigated using SAXS and rheology. Our main conclusions are as follows:

1. The micelle aggregation number increases with increasing gel concentration, and the average spacing between micelles is relatively insensitive to concentration changes. The relationship between the aggregation number and the polymer concentration depends strongly on the length of the endblocks. The degree of midblock stretching increases for gels with relatively large aggregation numbers and short midblocks.

2. SAXS experiments show a dramatic decrease in intensity over the same 20 °C temperature range where rheology shows gels transition from elastic to viscous behavior.

3. Master curves consistent with Maxwell-type relaxation with a fairly narrow range of relaxation times were obtained for three different triblocks over a large concentration range. The gels transition smoothly from nearly perfectly elastic behavior to viscous flow and have a fundamentally liquidlike relaxation spectrum. Time−temperature superposition was possible over the temperature regime where the decrease in SAXS intensity is observed. This result suggests that the rheological response is controlled by endblock association throughout the entire transition regime.

4. Relaxation times were found to depend strongly on gel concentration and endblock length. Increasing the endblock length from 9K to 25K increases the relaxation time of a gel with $\varphi_p = 0.15$ by a factor of 10^6. For a given triblock gel, the micelle aggregation number is highly correlated with the relaxation time.

5. The apparent activation energies describing the temperature dependence of the relaxation times were roughly identical for all polymers and concentrations studied. The very high effective activation energy of ∼550 kJ/mol is due to the strong temperature dependence of the interaction between the endblocks and the solvent. This single apparent activation energy describes the behavior over a 40 °C temperature range, where the relaxation times vary by a factor of 10^{10}. At higher temperatures, the strong temperature dependence levels off, and the viscosity of the triblock solutions parallels that of the neat solvent, indicating eventual dissolution of the endblock aggregates.

Acknowledgment. We are grateful to Kuraray Co. of Japan for providing the triblocks used in these studies and to Steven Weigand for all his help collecting the SAXS data. This material is based upon work supported under a National Science Foundation Graduate Research Fellowship and by the Northwestern University Materials Research Center, through the NSF MRSEC program DMR-0520513. Portions of this work were performed at the DuPont−Northwestern−Dow Collaborative Access Team (DND-CAT) Synchrotron Research Center located at Sector 5 of the Advanced Photon Source. DND-CAT is supported by the E.I. DuPont de Nemours & Co., The Dow Chemical Company, the U.S. National Science Foundation through Grant DMR-9304725, and the State of Illinois through the Department of Commerce and the Board of Higher Education Grant IBHE HECA NWU 96. Use of the Advanced Photon Source was supported by the U.S. Department of Energy, Office of Science, Office of Basic Energy Sciences, under Contract W-31-10.

References and Notes

(1) Spontak, R. J.; Patel, N. P. *Curr. Opin. Colloid Interface Sci.* **2000**, *5*, 334−341.
(2) Hotta, A.; Clarke, S. M.; Terentjev, E. M. *Macromolecules* **2002**, *35*, 271−277.
(3) Creton, C. *Mater. Res. Bull.* **2003**, *28*, 434−439.
(4) Sudarsan, A. P.; Wang, J.; Ugaz, V. M. *Anal. Chem.* **2005**, *77*, 5167−5173.
(5) Montgomery, J. K.; Botha, A. S.; Drzal, P. L.; Shull, K. R.; Faber, K. T. *Scr. Mater.* **2003**, *48*, 785−789.
(6) Montgomery, J. K.; Drzal, P. L.; Shull, K. R.; Faber, K. T. *J. Am. Ceram. Soc.* **2002**, *85*, 1164−1168.
(7) Drzal, P. L.; Shull, K. R. *J. Adhes.* **2005**, *81*, 397−415.
(8) Flanigan, C. M.; Crosby, A. J.; Shull, K. R. *Macromolecules* **1999**, *32*, 7251−7262.
(9) Kempe, M. D.; Scruggs, N. R.; Verduzco, R.; Lal, J.; Kornfield, J. A. *Nat. Mater.* **2004**, *3*, 177−182.
(10) Annable, T.; Buscall, R.; Ettelaie, R. *Colloids Surf., A* **1996**, *112*, 97−116.
(11) Berret Damien, C.; Collet, A.; Viguier, M. *Curr. Opin. Colloid Interface Sci.* **2003**, *8*, 296−306.
(12) Agrawal, S. K.; Sanabria-DeLong, N.; Tew, G. N.; Bhatia, S. R. *J. Mater. Res.* **2006**, *21*, 2118−2125.
(13) Drzal, P. L.; Shull, K. R. *Macromolecules* **2003**, *36*, 2000−2008.
(14) Annable, T.; Buscall, R.; Ettelaie, R.; Whittlestone, D. *J. Rheol.* **1993**, *37*, 695−726.
(15) Le Meins, J.-F.; Tassin, J.-F. *Colloid Polym. Sci.* **2003**, *281*, 283−287.
(16) Laurer, J. H.; Mulling, J. F.; Khan, S. A.; Spontak, R. J.; Bukovnik, R. *J. Polym. Sci., Part B: Polym. Phys.* **1998**, *36*, 2379−2391.
(17) Jackson, N. R.; Wilder, E. A.; White, S. A.; Bukovnik, R.; Spontak, R. J. *J. Polym. Sci., Part B: Polym. Phys.* **1999**, *37*, 1863−1872.
(18) Forster, S.; Plantenberg, T. *Angew. Chem., Int. Ed.* **2002**, *41*, 689−714.
(19) Matsen, M. W.; Bates, F. S. *Macromolecules* **1996**, *29*, 7641−7644.
(20) Matsen, M. W.; Thompson, R. B. *J. Chem. Phys.* **1999**, *111*, 7139−7146.
(21) Nie, H. F.; Bansil, R.; Ludwig, K.; Steinhart, M.; Konak, C.; Bang, J. *Macromolecules* **2003**, *36*, 8097−8106.
(22) Kleppinger, R.; Mischenko, N.; Reynaers, H. L.; Koch, M. H. J. *J. Polym. Sci., Part B: Polym. Phys.* **1999**, *37*, 1833−1840.
(23) Vega, D. A.; Sebastian, J. M.; Loo, Y. L.; Register, R. A. *J. Polym. Sci., Part B: Polym. Phys.* **2001**, *39*, 2183−2197.
(24) Reynders, K.; Mischenko, N.; Kleppinger, R.; Reynaers, H.; Koch, M. H. J.; Mortensen, K. *J. Appl. Crystallogr.* **1997**, *30*, 684−689.

(25) Ferry, J. D. *Viscoelastic Properties of Polymers*, 3rd ed.; John Wiley & Sons: New York, 1980.
(26) Raspaud, E.; Lairez, D.; Adam, M.; Carton, J. P. *Macromolecules* **1996**, *29*, 1269−1277.
(27) Kim, S. H.; Jo, W. H. *Macromolecules* **2001**, *34*, 7210−7218.
(28) Nguyenmisra, M.; Mattice, W. L. *Macromolecules* **1995**, *28*, 1444−1457.
(29) Watanabe, H.; Sato, T.; Osaki, K. *Macromolecules* **2000**, *33*, 2545−2550.
(30) Semenov, A. N.; Joanny, J. F.; Khokhlov, A. R. *Macromolecules* **1995**, *28*, 1066−1075.
(31) Leibler, L.; Orland, H.; Wheeler, J. C. *J. Chem. Phys.* **1983**, *79*, 3550−3557.
(32) Nagarajan, R.; Ganesh, K. *J. Chem. Phys.* **1989**, *90*, 5843−5856.
(33) Prochazka, O.; Tuzar, Z.; Kratochvil, P. *Polymer* **1991**, *32*, 3038−3044.
(34) Raspaud, E.; Lairez, D.; Adam, M.; Carton, J. P. *Macromolecules* **1994**, *27*, 2956−2964.
(35) Wijmans, C. M.; Eiser, E.; Frenkel, D. *J. Chem. Phys.* **2004**, *120*, 5839−5848.
(36) Lairez, D.; Adam, M.; Carton, J. P.; Raspaud, E. *Macromolecules* **1997**, *30*, 6798−6809.
(37) Alexandridis, P.; Hatton, T. A. *Colloids Surf., A* **1995**, *96*, 1−46.
(38) Bansil, R.; Nie, H.; Li, Y.; Liao, G.; Ludwig, K.; Steinhart, M.; Konak, C.; Lal, J. *Macromol. Symp.* **2002**, *190*, 161−172.
(39) Mischenko, N.; Reynders, K.; Koch, M. H. J.; Mortensen, K.; Pedersen, J. S.; Fontaine, F.; Graulus, R.; Reynaers, H. *Macromolecules* **1995**, *28*, 2054−2062.
(40) Tanaka, F.; Edwards, S. F. *Macromolecules* **1992**, *25*, 1516−1523.
(41) Pham, Q. T.; Russel, W. B.; Thibeault, J. C.; Lau, W. *Macromolecules* **1999**, *32*, 5139−5146.
(42) Castelletto, V.; Hamley, I. W.; Yuan, X.-F.; Kelarakis, A.; Booth, C. *Soft Matter* **2005**, *1*, 138−145.
(43) Inomata, K.; Nakanishi, D.; Banno, A.; Nakanishi, E.; Abe, Y.; Kurihara, R.; Fujimoto, K.; Nose, T. *Polymer* **2003**, *44*, 5303−5310.
(44) Percus, J. K.; Yevick, G. J. *Phys. Rev.* **1958**, *110*, 1−13.
(45) Kinning, D. J.; Thomas, E. L. *Macromolecules* **1984**, *17*, 1712−1718.
(46) Laurer, J. H.; Mulling, J. F.; Khan, S. A.; Spontak, R. J.; Lin, J. S.; Bukovnik, R. *J. Polym. Sci., Part B: Polym. Phys.* **1998**, *36*, 2513−2523.
(47) Milner, S. T. *Macromolecules* **2005**, *38*, 4929−4939.
(48) Lakrout, H.; Creton, C.; Ahn, D. C.; Shull, K. R. *Macromolecules* **2001**, *34*, 7448−7458.
(49) Laurer, J. H.; Khan, S. A.; Spontak, R. J.; Satkowski, M. M.; Grothaus, J. T.; Smith, S. D.; Lin, J. S. *Langmuir* **1999**, *15*, 7947−7955.
(50) Winter, H. H.; Chambon, F. *J. Rheol.* **1986**, *30*, 367−382.
(51) Macosko, C. W. *Rheology: Principles, Measurements, and Application*; Wiley-VCH: New York, 1994.
(52) Baumgaertel, M.; Schausberger, A.; Winter, H. H. *Rheol. Acta* **1990**, *29*, 400−408.
(53) Yu, J. M.; Jerome, R. *Macromolecules* **1996**, *29*, 8371−8378.
(54) Wilder, E. A.; White, S. A.; Smith, S. D.; Spontak, R. J. Gel network development inn AB, ABA, and AB/ABA block copolymer solutions inn a selective solvent. In *Polymer Gels: Fundamentals and Applications*, 2003; Vol. 833, pp 248−261.
(55) Ellison, C. J.; Kim, S. D.; Hall, D. B.; Torkelson, J. M. *Eur. Phys. J. E* **2002**, *8*, 155−166.

MA061993+